Atmospheric Environment 319 (2024) 120285

Contents lists available at ScienceDirect

Atmospheric Environment

journal homepage: www.elsevier.com/locate/atmosenv

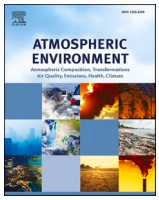

Impact of the COVID-19 lockdown to a port-city area: A two-year comparative PMF analysis of PM_{10} of polluting sources

D. Tobarra [a,*], E. Yubero [b], Á. Clemente [b], A. Carratala [a]

[a] Department of Chemical Engineering, University of Alicante, P. O. Box 99, 03080, Alicante, Spain
[b] Atmospheric Pollution Laboratory (LCA), Department of Applied Physics, Miguel Hernández University, Avenida de la Universidad S/N, 03202, Elche, Spain

HIGHLIGHTS

- Positive Matrix Factorization was used to identify the Impact of the COVID-19 lockdown to PM_{10} sources a port-city area.
- The reduction of PM_{10} from road traffic was limited to the COVID lockdown, while that from marine traffic is year-round.
- The increase in the Saharan source compensates the reduction in PM_{10} caused by anthropogenic sources during the COVID year.

ARTICLE INFO

Keywords:
PM_{10}
Positive matrix factorization
COVID-19
Lockdown
Port
Source apportionment

ABSTRACT

The objective of this study was to evaluate the effects that the COVID-19 lockdown had in the PM_{10} levels and sources in a city adjacent port where the transport of bulk materials is one of the main activities. For this, the 2020 PM_{10} chemistry and sources will be compared to an annual baseline period of 2017-18 in the same area.

A total of 337 samples were chemically analyzed (30 chemical species) and a positive matrix factorization model was used to identify major PM_{10} sources. A Mann-Whitney test was used to find statistically relevant differences between periods.

The model identified 8 factors two of them directly related to port activities (Shipping emissions and bulk materials), one associated to road traffic, three linked secondary sources (aged sea salt, secondary nitrate, ammonium sulfate) and two natural sources including fresh sea salt and long-range transport from Saharan intrusions.

Road traffic and Shipping sources show a significant reduction in the lockdown period. However, after this period, the road traffic source quickly recovered showing no differences on a yearly basis with the reference year. Only the Shipping emissions source were greatly reduced in 2020 compared to 2017-18. On the other hand, the influence of natural sources kept PM_{10} from reducing drastically during the lockdown year (2020).

1. Introduction

PM_{10} particles are a worldwide concern, with several studies highlighting health effects in humans (Cheng et al., 2013; Khaniabadi et al., 2017; Sasmita et al., 2022) and particularly in children (Johnson et al., 2021; Mahapatra et al., 2020; Nauwelaerts et al., 2022). A large number of studies in exposed human populations over decades show associations between prenatal exposure to fine particulate matter (PM) and adverse birth outcomes, respiratory disease, and adverse neurodevelopment (Johnson et al., 2021). Most International organizations (World Health Organization, European Environment Agency) and national organizations (United States Environmental Protection Agency), have set different limit values for key pollutants to protect the health of their citizens. These limits are used as targets for reducing emissions. Air quality measurement is essential to detect the exceedances of the daily limit value for PM_{10} set by Directive (2008)/50/EC (50 $\mu g/m^3$), while the World Health Organization recommends a lower limit value for PM_{10} (15 $\mu g/m^3$) (WHO; 2021). The identification of the main sources, in environments affected by the presence of industrial ports, contributing to PM has become necessary to reduce their negative impact on air quality (Cheng et al., 2013; Merico et al., 2017; Oduber et al., 2021; Pérez et al., 2016; Russo et al., 2018; Sasmita et al., 2022; Viana et al., 2009; Wu et al., 2013; Zhou et al., 2015).

Ports are very important to the global economy, as they facilitate

* Corresponding author.
E-mail address: daniel.tobarra@ua.es (D. Tobarra).

https://doi.org/10.1016/j.atmosenv.2023.120285
Received 17 July 2023; Received in revised form 15 November 2023; Accepted 6 December 2023
Available online 10 December 2023

international trade and are considered to be major accelerators of local economic development by providing low-cost means of transporting goods with far away regions. In addition, they are very relevant to the growth of the cities in which they are located (Ma et al., 2021; Notteboom et al., 2022). However, maritime transport pollutes the sea and the air by emitting gases and particles. In the case of particles, the handling of bulk materials in ports contributes to increased levels of PM_{10} and $PM_{2.5}$ in the area (Alastuey et al., 2007; Clemente et al., 2021; Pérez et al., 2016), however, identifying the bulk material source is often challenging due to its composition's similarity to the soil, leading to it being labeled as a general mineral source. On the other hand, emissions from ships, mainly represented by combustion of fuel-oil have been well documented by different studies which found their contribution between 0.3% and 7% of the total PM_{10} (Alastuey et al., 2007; Amato et al., 2009; Clemente et al., 2021; Ledoux et al., 2018; Merico et al., 2017; Pandolfi et al., 2010; Pérez et al., 2016; Viana et al., 2009). Traffic in the port area cannot be underestimated as most of the vehicles passing through the area are heavy duty vehicles carrying both bulk materials and containers.

In 2020, the COVID-19 pandemic caused a 3-month lockdown that greatly reduced anthropogenic emissions, mainly those related to road traffic. This period has already been studied in detail to see what influence it has had on particulate levels (Gayen et al., 2021; Millán-Martínez et al., 2021; Shukla et al., 2022). Many studies have focused on the effects of COVID-19 closures directly on the road traffic source, NOx or PM_{10} (Collivignarelli et al., 2020; Dantas et al., 2020; Massimi et al., 2022; Millán-Martínez et al., 2022; Sharma et al., 2020; Xu et al., 2020). However, few studies have focused on the effects of the lockdowns in port cities where maritime transport of goods and cruise ships are important contributors to PM_{10}.

The aim of this study is to evaluate the effects of the lockdown caused by the COVID-19 pandemic in the PM_{10} concentrations in a city adjacent to a port where the transport of bulk materials is one of the main activities. To achieve this, two periods were studied in the same sampling area in Alicante (a city in the south-east of Spain), the full year of 2020 and the period from March 2017 to February 2018 (hereafter referred to as 2017 and used as reference). A PMF model is used to study the effect the lockdown may have had on PM_{10} concentrations, composition and sources, as well as how emission patterns have changed during 2020.

2. Materials and methods

2.1. Measuring site

The monitoring station, named TF (Tinglado Frutero), is located at the perimeter of the port of Alicante (38° 20′ 13″ N; 0° 29' 48" O), between the bulk solids handling docks (D-11, D-13 and D-17) and the urban area of Alicante (Fig. 1). The distances from the sampling point to dock D-17 is 400m, 590m to D-13 and 740m to D-11. Moreover, the largest dock (D-17) is less than 600m away from the city boundary where a public school is located. The location of the sampling point was chosen at the boundary between the port and the urban area, in order to minimize proximity to emission sources while staying close to the residential part of the city.

The port is the south-eastern window to the Mediterranean Sea of a semi-arid basin surrounded by mountains where the recirculation of pollutants is favored for most of the year (Clemente et al., 2022). The climatology is characterized by short and mild winters for two months (January–February), followed by a long warm period dominated by local thermal circulations and sea breezes (Santacatalina et al., 2011; Yubero et al., 2015). The annual precipitation is less than 300 mm (220 mm in 2017 and 190 in 2020) and occurs in very few events. The number of days without precipitation, <0.1 mm, is greater than 300 which enhances the existence of dry bare soils and facilitates particle resuspension. The high frequency of Saharan episodes is also common in the study area and could be variable between years. For instance, 60 relevant episodes occurred in 2020 compared to 40 in 2017. In Fig. 2, the seasonal wind roses for the study periods show the seasonality of the winds and the low variation from year to year. With this wind regime, port emissions would affect the sampling point during periods of winter stability and, in the summer, during daytime hours with E-S winds (up to 10 m/s) as well as during nighttime hours with light winds or stability. The number of days with high stability resulting in PM_{10} levels above 40 $\mu g/m^3$, was 23 in 2020 and 15 in the reference period.

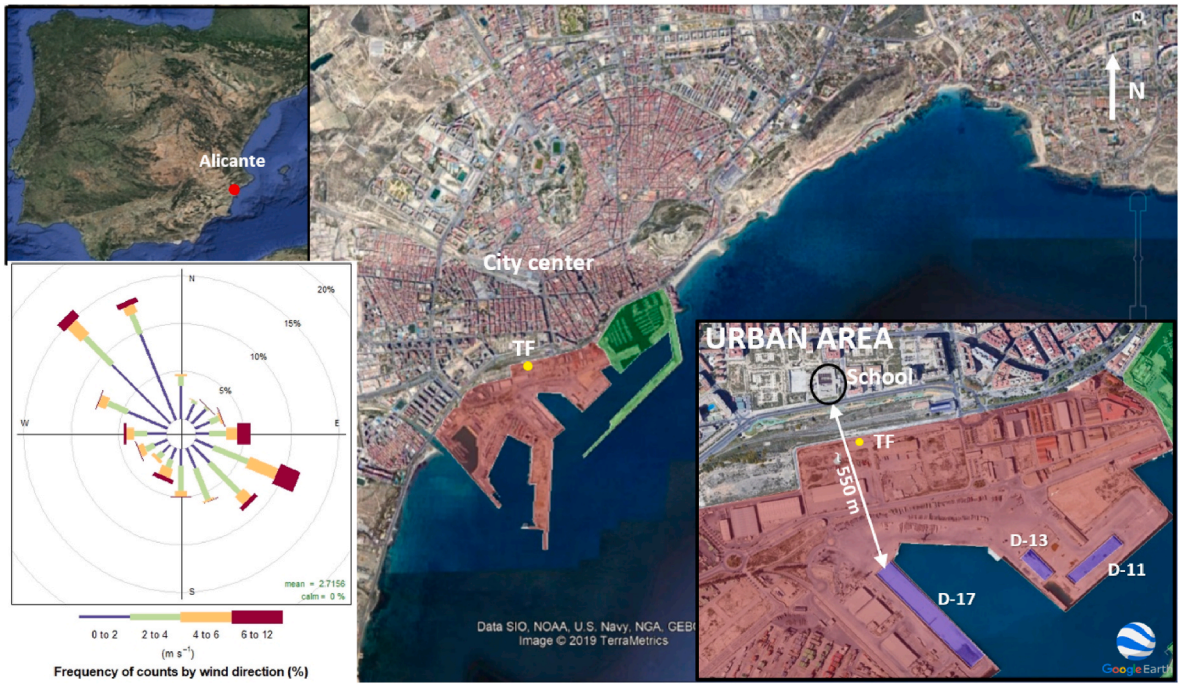

Fig. 1. Location of the measurement point (TF) and average wind rose (2020). The industrial area of the harbor of Alicante is shaded in red while the sports and leisure area is shaded in green. The docks where solid bulk materials are handled are shaded in purple. Figure adapted from Clemente et al., (2021).

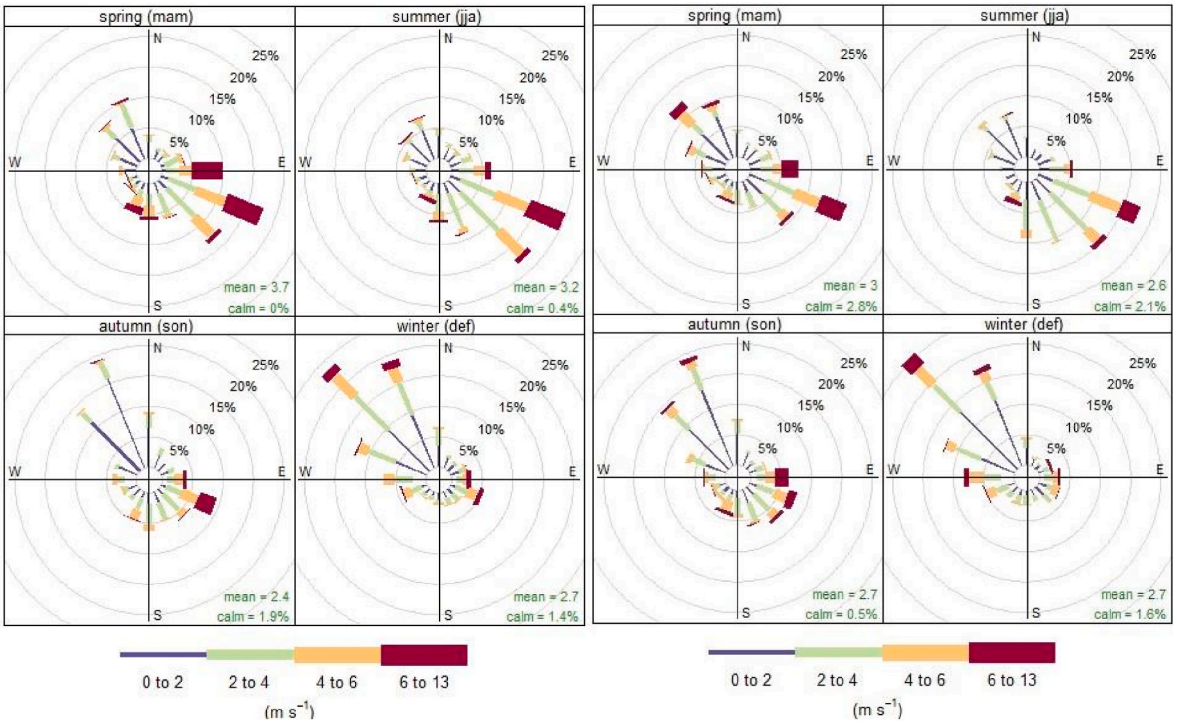

Fig. 2. Seasonal windroses for the study period. 2017 on the left, 2020 on the right. Calms are winds under 0.5 m/s.

The average annual amount of bulk materials handled in the Port of Alicante over the last 10 years was 1.28 ± 0.44 million tonnes. In 2020, 1.4 million tonnes of bulk materials were handled, in comparison to the 1.9 million tonnes recorded in 2017, the year with the highest bulk movement. (Autoridad Portuaria de Alicante, 2021).

To mitigate the impacts that port activity may have on atmospheric particulate matter concentration, the Port Authority has implemented a monitoring system based on continuous PM measurements. Once certain thresholds are exceeded, various additional abatement techniques are activated alongside the existing barriers, such as the use of water cannons, and all activity is halted if the levels do not decrease.

2.2. Sample collection and analysis

During 2020 and 2017, a total of 156 and 181 PM_{10} samples were collected respectively on alternate days with a high-volume sampler (DIGITEL DHA-80) installed on the roof of an approximately 2.5m high freight container located at the monitoring site (TF). Sampling was performed using Munktell micro-quartz fiber filters (ø = 150 mm) and each filter was sampled for 24h starting at 00:00 on alternate days.

Filters were conditioned in a room with controlled temperatures (20 ± 1 °C) and relative humidity (50 ± 5%) for 48h before each weighing. The mass of the collected particles was determined by the difference between the weight of the filter before and after the sampling. An electronic scale (Ohaus, Analytical Plus, AP250D) with 10 μg sensitivity was employed.

The 337 samples were analyzed by ion chromatography (IC, Dionex ICS-1100), thermal optical transmission analysis (TOT, Sunset Laboratory, Inc.), inductively coupled plasma optical emission spectroscopy (ICP-OES, Optima 7300 DV) and ICP mass spectrometry (ICP-MS, 7700x Agilent) to quantify soluble ions, carbonaceous compounds and elements (major and trace). For that, filters have been fractioned, a water extraction was realized in the case of soluble ions and a ($HNO_3 + H_2O_2$) digestion was realized for total metals. EC-OC has been conducted in a punch (1.5 cm^2) of the filter. Carbonates were assumed to be those that complete the ionic balance (Yubero et al., 2010). A more detailed explanation of the analytical methodology followed and the detection limits can be found elsewhere (Clemente et al., 2021; Galindo, N. et al., 2018; Galindo et al., 2018; Galindo and Yubero, 2017).

Blank filters were analyzed with each batch of filters using the respective analytical techniques. The average concentration values for each species in the blank were subtracted from the concentration of the analyzed samples. The detection limit was obtained as 3 times the standard deviation of the blanks that correspond to the filter.

2.3. PMF

The Positive Matrix Factorization (PMF) technique (Paatero and Tapper, 1994) was employed to carry out the source apportionment at the monitoring site from the chemical composition of the analyzed samples, by means of the EPA (Environmental Protection Agency) PMF version 5.0. The PMF model is commonly used for PM source identification and apportionment (Amato et al., 2009; Clemente et al., 2021; Jaeckels et al., 2007; Kim and Hopke, 2008; Kim et al., 2004; Larsen and Baker, 2003; Lee, E. et al., 1999; Lee, P. K. H. et al., 2003; Maykut et al., 2003; Pandolfi et al., 2010).

The data from the 2017 and 2020 periods were merged to help with the factor identification and to better compare changes in sources contributing to the PM_{10} study area.

A total of 30 chemical species were used for the source apportionment analysis, of which 11 were classified as strong (Cl^-, NO_3^-, NH_4^+, Mg^{2+}, Ca^{2+}, Al, V, K, Fe, Na^+ and EC) and 19 as weak (PM_{10}, SO_4^{2-}, $C_2O_4^{2-}$, Ti, Cr, Mn, Ni, Cu, As, Sr, Zr, Sn, Sb, Ba, La, Ce, Pb, and OC).

This classification was done in two steps, the first one being mainly based on their signal-to-noise ratio (S/N; Paatero and Hopke, 2003). Species with a S/N > 2 were initially classified as strong while those with a S/N between 0.2 and 2 were classified as weak and those with a S/N < 0.2 were classified as bad. Of the species originally classified as strong, some were changed to weak because a low percentage of the samples were above the detection limit or to improve the stability of the Q factor.

Concentration values below the detection limit were replaced by half the detection limit and missing values were replaced by the species mean value (Polissar et al., 1998). The uncertainty associated with each

concentration value was calculated using the equations proposed by Zabalza et al. (2006).

A range of 5–10 factors were tested on the PMF, all runs were performed with an additional 5% uncertainty. Diagnostic tests such as bootstrap (BS) and displacement (DISP) were performed to evaluate the rotational ambiguity, the uncertainty of the model and the stability of the solution. (Belis et al., 2014; Comero et al., 2009).

2.4. Mann-Whitney test

A Mann-Whitney test ($\alpha = 0.05$) was applied to the different factors obtained by the PMF to compare the 2017 period with the 2020 period and to determine whether there were statistically significant differences between them.

3. Results

3.1. Average composition of PM_{10}

The average PM_{10} concentration in 2020, the COVID year, was 29.1 ± 17.8 μg/m^3, which was not statistically different from the average obtained at the same sampling point in 2017 (Table 1). In 2020, the higher PM_{10} concentration was obtained on February 28th due to a Saharan intrusion where the concentration peaked at 175.9 μg/m^3. The lower concentration, with a value of 7.8 μg/m^3, was measured on December 5th with a strong Atlantic advection episode.

The number of exceedances of the PM_{10} daily limit value established by Directive (2008)/50/EC (50 μg/m^3) regulations was 7 and 8 days in 2017 and 2020, respectively. Regarding the total number of sampled days, the percentage of exceedances, 4.5%, is similar in both periods.

Table 1 summarizes the average composition of PM_{10} in 2020 and 2017. In 2020, OC (4.7 μg/m^3) is the major mass fraction followed by NO_3^- (2.8 μg/m^3), and SO_4^{2-} (2.2 μg/m^3). In 2017 the pattern was similar, 4.6, 2.4 and 2.6 μg/m^3 for OC, SO_4^{2-} and NO_3^- respectively. Most of the samples have almost 100% of their values above the detection limit. Statistical analysis shows that there is a significant difference for V, Ni, Zr, Fe, Sb, Cr, Ti, EC and $C_2O_4^{2-}$ in both periods. V and Ni are commonly associated with fuel-oil combustion and therefore this reduction could imply a decline in maritime transport. Fe, Sb, Cr and EC are usually related to road traffic (Amato et al., 2009; Maykut et al., 2003) which showed an important reduction in 2020. Ti and Fe, on the other hand, are main tracers of Saharan intrusions. $C_2O_4^{2-}$ is mainly a tracer of secondary processes (Huang et al., 2011; Zhou et al., 2015).

The sum of the individual concentration for all the elements has been compared to the PM_{10} for both periods (2017, 2020). The calculated PM_{10} obtained by the chemical composition represents 80% and 82% of the total PM_{10} sampled, respectively. The missing 18–20% are related to aerosol-bound water, minor non-analyzed chemical components, non-measured oxygen in OC and metals and small instrumental errors (Cardoso et al., 2018; Santacatalina et al., 2010; Vecchi et al., 2008; Wu et al., 2013).

The measured annual average PM_{10} concentration (29 μg/m^3) is lower than other more industrialized ports in Spain such as Tarragona (40 μg/m^3; Alastuey et al., 2007) or Barcelona (35 μg/m^3; Pérez et al., 2016). Compared to other European ports, the concentration is slightly higher than that of the Port of Calais, France (25 μg/m^3; Ledoux et al., 2018), and half of that of the lagoon in Venice, Italy (62 μg/m^3, Merico et al., 2017).

The port of Alicante has lower concentration of trace metals and main ions like SO_4^{2-} and NH_4^+ than larger ports such as Barcelona and Tarragona. The levels of V and Ni, are either lower than other ports or on the lower end, especially for 2020 (2–15.3 ng/m^3, 1.9–7.3 ng/m^3 for V and Ni respectively). Although elements related to fuel-oil combustion and therefore the number of ships docking at the port are relatively less significant than in larger ports, the concentrations of NO_3^-, Na^+, Cl^- and Ca^+ are of the same order compared to those ports (2.4–7.0 μg/m^3,

Table 1
Summary PM_{10} concentration and chemical composition in the Port of Alicante. Maximum, minimum and mean concentrations of the 156 samples of the 2020 period and the 181 samples of the 2017 period with their standard deviation (SD) and the percentage of values above the detection limit (ADL).

	Species	2020					2017				
		Mean	Max	Min	SD	ADL (%)	Mean	Max	Min	SD	ADL (%)
μg/m^3	PM_{10}	29.1	175.9	7.8	17.8	100%	28.5	120	5.8	15.7	100%
	Cl^-	1.0	7.8	0.02	1.2	95%	0.93	5.2	0.06	0.82	96%
	NO_3^-	2.8	12.7	0.14	2.2	99%	2.4	9.0	0.17	1.5	100%
	SO_4^{2-}	2.2	6.4	0.40	1.3	99%	2.6	8.2	0.15	1.7	100%
	$C_2O_4^{2-}$	0.31	0.70	0.05	0.14	99%	0.20	0.6	<0.01	0.10	100%
	NH_4^+	0.22	5.8	<0.01	0.60	73%	0.22	2.1	<0.01	0.30	99%
	Fe	0.42	2.6	0.07	0.35	86%	0.30	1.4	0.05	0.23	100%
	Na^+	1.21	4.6	0.04	0.97	94%	1.1	4.3	0.11	0.75	98%
	Mg^{2+}	0.18	0.56	0.02	0.12	96%	0.16	0.5	0.03	0.09	100%
	Ca^{2+}	1.8	6.5	0.37	0.99	100%	2.1	11.3	0.22	1.6	100%
	K^+	0.35	3.3	0.07	0.32	99%	0.33	1.4	0.07	0.20	100%
	Al	0.32	4.2	0.05	0.47	99%	0.35	1.5	0.04	0.22	91%
	CO_3^{2-}	1.4	5.9	<0.01	0.85	100%	1.8	11.4	0.07	1.7	100%
	OC	4.7	10.9	2.6	1.8	100%	4.6	13.5	2.2	1.9	100%
	EC	0.95	8.0	0.18	0.79	100%	0.73	2.9	0.15	0.40	100%
ng/m^3	Ti	10.8	49.2	1.0	9.3	99%	9.7	87.7	1.1	10.3	100%
	V	3.3	22.2	0.22	3.6	99%	7.9	50.4	0.45	7.0	100%
	Cr	3.0	34.7	<0.01	4.1	89%	4.2	18.5	1.81	3.2	59%
	Mn	6.5	47.5	1.2	6.0	100%	6.5	31.3	1.2	3.9	100%
	Ni	2.0	12.2	0.14	1.6	89%	3.8	17.1	0.60	2.8	94%
	Cu	8.8	35.2	1.2	6.1	99%	13.4	108	2.8	11.2	100%
	As	0.30	1.2	0.05	0.19	99%	0.35	1.1	0.07	0.22	70%
	Sr	7.5	34.6	1.8	5.6	99%	8.2	39.0	1.2	6.4	100%
	Zr	1.5	12.5	0.12	1.4	98%	4.2	20.4	0.78	3.7	54%
	Sn	1.7	6.3	0.22	1.2	99%	2.1	9.9	0.43	1.5	97%
	Sb	0.62	2.2	<0.01	0.40	99%	1.74	10.9	0.26	1.47	97%
	Ba	13.4	97.2	0.86	11.2	99%	15.0	85.6	3.54	11.1	88%
	La	0.33	7.3	0.05	0.63	99%	0.24	0.9	0.05	0.16	100%
	Ce	0.61	15.1	0.05	1.3	99%	0.42	1.7	0.08	0.3	100%
	Pb	3.1	14.7	0.1	2.6	99%	4.1	49.8	0.5	5.6	100%

0.69–1.9 μg/m^3, 0.13–2.9 μg/m^3 and 1.1–2.5 μg/m^3 respectively; Alastuey et al., 2007; Amato et al., 2009; Pandolfi et al., 2010; Pérez et al., 2016; Strak et al., 2011; Wu, G. et al., 2013; Wu, S. et al., 2020; Žitnik et al., 2005). The levels of Na^+ and Cl^- more related with regional oceanic emissions and proximity to the sea shore also are in the range of Mediterranean ports (0.69–1.9 μg/m^3, 0.13–2.9 μg/m^3; Alastuey et al., 2007; Amato et al., 2009; Pandolfi et al., 2010; Pérez et al., 2016; Strak et al., 2011; Wu, G. et al., 2013; Wu, S. et al., 2020; Žitnik et al., 2005).

The OC/EC ratios were calculated from individual samples by subtracting the carbon corresponding to carbonates from OC, resulting in values of 5.8 and 6.5 during 2020 and 2017, respectively. Additionally, it was observed that in 2017, the ratios were higher during the winter period compared to the summer period, indicating a greater biomass burning relative to traffic emissions in winter for (Szidat et al., 2006).

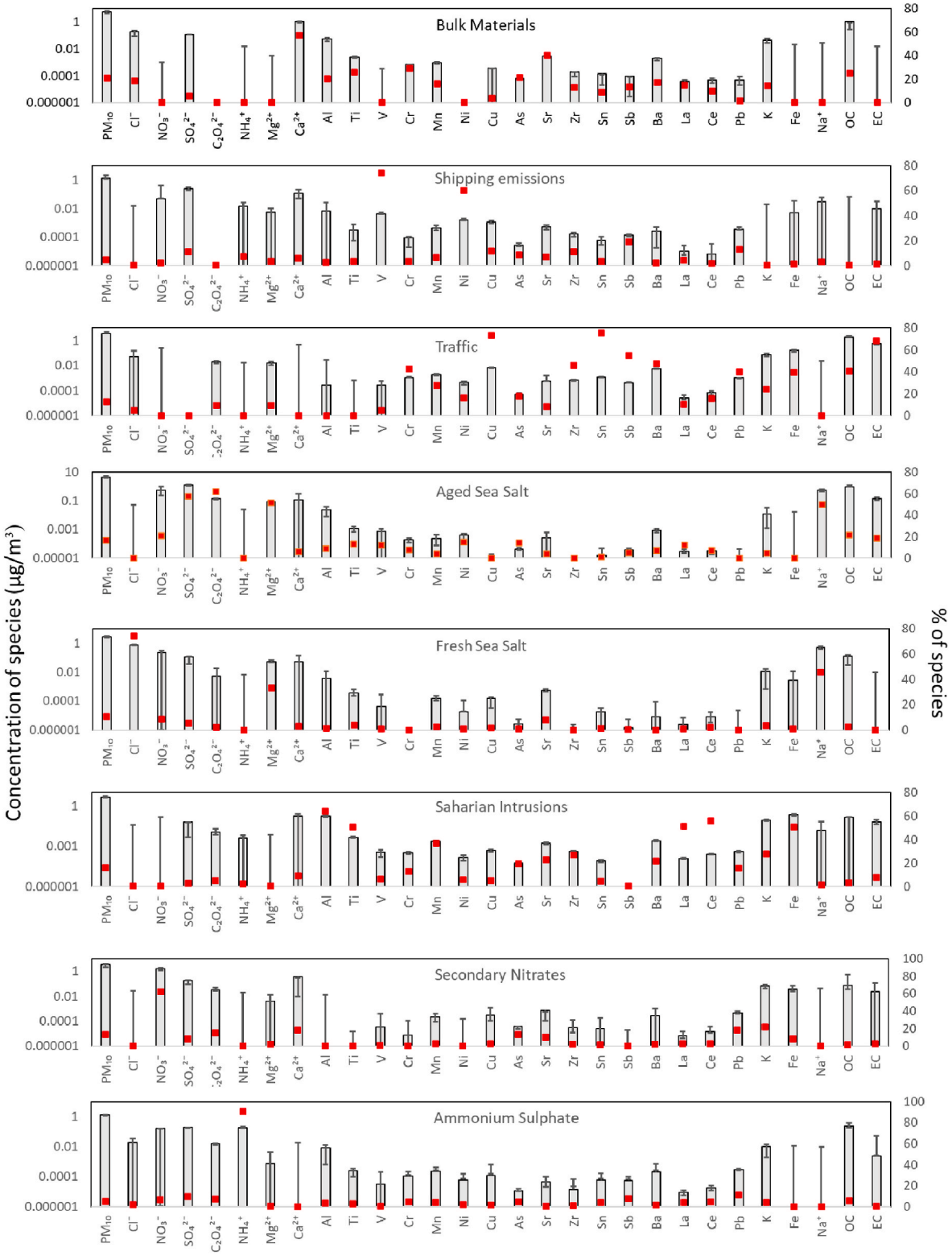

Fig. 3. Chemical profiles of the identified PMF factors. Error bars show DISP-Min and DISP-Max.

3.2. Source apportionment

To obtain which are the main sources contributing to the PM_{10} concentration at the sampling point and to see how they have changed between the two study periods, a PMF is performed including the data from both periods. The merging of the two databases (2017 and 2020) allowed for a better identification of the factors and comparison among years.

The stability of the Q value was checked for each number of factors while the suitability of the solutions was evaluated by focusing on the analysis of the scaled residuals, the observed versus predicted scatter plots and the G-space plots (Belis et al., 2014; Comero et al., 2009). The chosen solution consists of 8 factors, as adding a 9th factor would result in the splitting of the traffic factor into two nearly equal components, lacking any physicochemical significance. However, with 7 factors, the Saharan intrusion factor disappears and is distributed amongst the other factors. The highest stability of the Q was found with this number of factors. The scaled residuals were distributed between −3 and +3 for almost all species. No factor swaps took place during DISP for dQmax values of 4 and 8.

The chemical profiles of the identified PMF factors are shown in Fig. 3. Fig. 4 shows the temporal evolution of each factor contribution to PM_{10} in the two periods of study. For a better comparison, in the case of the 2017 period, January and February 2018 are represented as if they were from 2017. There was a good correlation between PM concentrations simulated by PMF and the sum of the quantified components ($R^2 = 0.92$) and 98% of the quantified PM_{10} was simulated in the analysis. Also, in Fig. 5, the PMF factor contribution (μg/m^3) to PM_{10} annual average for 2020 and 2017 is compared. The significance of the differences between both periods will be addressed in a specific section. The different factors obtained from the PMF were:

3.2.1. Bulk materials

This source, which represents 21% of the annual average of PM_{10}, is characterized mainly by Ca^{2+} (57%), with organic carbon (OC) (25% of explained variation) which includes carbonates and a mixture of almost all metals with a reasonable explained variation (10%–40%). This source includes limestone, clinker and gypsum, which are the materials most frequently transported in the Port of Alicante. The annual evolution of this source shows a baseline of around 5–10 μg/m^3 with peaks corresponding to days when limestone was handled in the port. In 2017, those peaks were more frequent and of higher intensity. This source contributed 6.7 μg/m^3 and 4.8 μg/m^3 to total PM during 2017 and 2020, respectively. Other studies include this source in a more general mineral source which includes Saharan intrusions, soil resuspension or other mineral sources on top of bulk materials. These factors typically range between 7 μg/m^3 and 10 μg/m^3 (Alastuey et al., 2007; Clemente et al., 2021; Pandolfi et al., 2010; Pérez et al., 2016).

3.2.2. Shipping emissions: fuel-oil

The contribution of this source to the PM_{10} is 5% and is mainly represented by two chemical components, V and Ni (75% and 60% of the explained variation respectively) with a ratio V/Ni = 2.6 and some SO_4^{2-} (12%). The ratio obtained is similar to that obtained in other articles for sources representing fuel-oil combustion from ships (Clemente et al., 2021; Pandolfi et al., 2010; Pérez et al., 2016; Viana et al., 2009). Shipping emissions include both maritime transport of goods and recreational vessels like cruise ships. This source would also include emissions from large freight ships traveling along the Mediterranean corridor located 40 km from the coast and, consequently, the sampling point. On many of the days when the contribution of this source is relevant, it can be seen, through an analysis of the back trajectories, that the air masses come from the east, i.e. from the Mediterranean. While during winter, prevailing winds from the NW direction restricted these emissions from reaching the monitoring area.

3.2.3. Road traffic

Road traffic contributes 13% to the PM_{10} mass concentration, represented by Cu (72%), Zr (46%), Sn (75%), Sb (55%) and Ba (48%), which are usually associated with brake and pad wear (Grigoratos and Martini, 2014; Pant and Harrison, 2013), and EC (69%), a clear marker of tailpipe exhaust (Megido et al., 2016; Sharma et al., 2014). As expected from this factor, weekdays have a significant higher contribution to PM_{10} than weekends (4.0 μg/m^3 and 2.5 μg/m^3 respectively) and levels are higher in winter periods (5.3 μg/m^3) than in the summer (2.3 μg/m^3) mainly due to the reduction in the height of the mixing layer and the lower dispersive conditions of the atmosphere. Due to the COVID-19 lockdown, traffic emissions were greatly reduced from March 15th to June 7th, and then began to slowly increase to reach levels similar to those at the beginning of the year. The effect of the COVID on the road traffic will be further investigated in a separate section.

3.2.4. Aged sea salt

Aged sea salt accounts for 16% of the total PM_{10} (4.5 μg/m^3), mainly represented by Na^+ (50%), $C_2O_4^{2-}$ (62%), SO_4^{2-} (57%) and Mg^{2+} (52%). The absence of Cl^-, and the presence of sulfate and some nitrate can be explained by the reactions between the NaCl particles and the gases present in the atmosphere such as HNO_3 and H_2SO_4 (Oduber et al., 2021; Song and Carmichael, 1999; Yubero et al., 2010).

Higher values during the summer period due to the reactions being favored by higher temperatures, solar radiation, and long periods of sea breeze contributed to an increase in aged sea salt levels from 1.7 μg/m^3 and 2.7 μg/m^3 in winter of 2017 and 2020 respectively to 7.3 μg/m^3 and 8.0 μg/m^3 in the summer of 2017 and 2020. This source becomes one of the most important during the summer months, contributing 29% of PM_{10}.

3.2.5. Fresh sea salt

This factor represents 10% of the annual average of PM_{10} and contains mainly Na^+ (46%), Mg^{2+} (33%) and Cl^- (74%). This factor was identified as fresh sea salt because the ratio of Na^+ to Cl^- is 1.47, which is close to the stoichiometric ratio for NaCl (1.54). The Na/Mg ratio is 8.9, which is also close to that of seawater (8.3; Yubero et al., 2010).

This factor mainly differs from aged sea salt mainly due to the presence of Cl^-. This means that this source is related to recently emitted sea spray that has not yet reacted with the nitric and sulfuric acids of the atmosphere. The days when this factor shows high levels correspond with strong advective episodes from the SE without recirculation of air masses.

3.2.6. Saharan intrusion

Saharan intrusion accounts for 16% of the total PM_{10} (4.5 μg/m^3) and is mainly represented by metals such as Al (64%), Ti (51%) and Fe (51%). This factor, unlike most of the others, has an almost negligible contribution for most of the year, except on intrusion days when its concentration increases significantly. The intrusion days obtained by the PMF model have been confirmed by meteorological intrusion models and the use of back-trajectory analysis to confirm the origin of the source.

3.2.7. secondary nitrates

The secondary nitrates contributed to 13% of the total PM_{10} mass concentration and primarily consisted of NO_3^- (62%), Ca^{2+} (18%) and K^+ (22%). This factor mainly represents calcium nitrate and potassium nitrate, which can be the result of the neutralization of nitric acid by basic species, mainly calcium, which is predominant in the area. Due to the small amount of ammonia present in the atmosphere, nitric acid reacts with calcium and potassium carbonates conforming of this source. This factor could be related with NO_2 emissions (HNO_3 precursor) from road and maritime traffic. The days on which this factor has the highest levels correspond to accumulation episodes. During these episodes, which occur mainly in winter, nitric acid and basic species tends to accumulate.

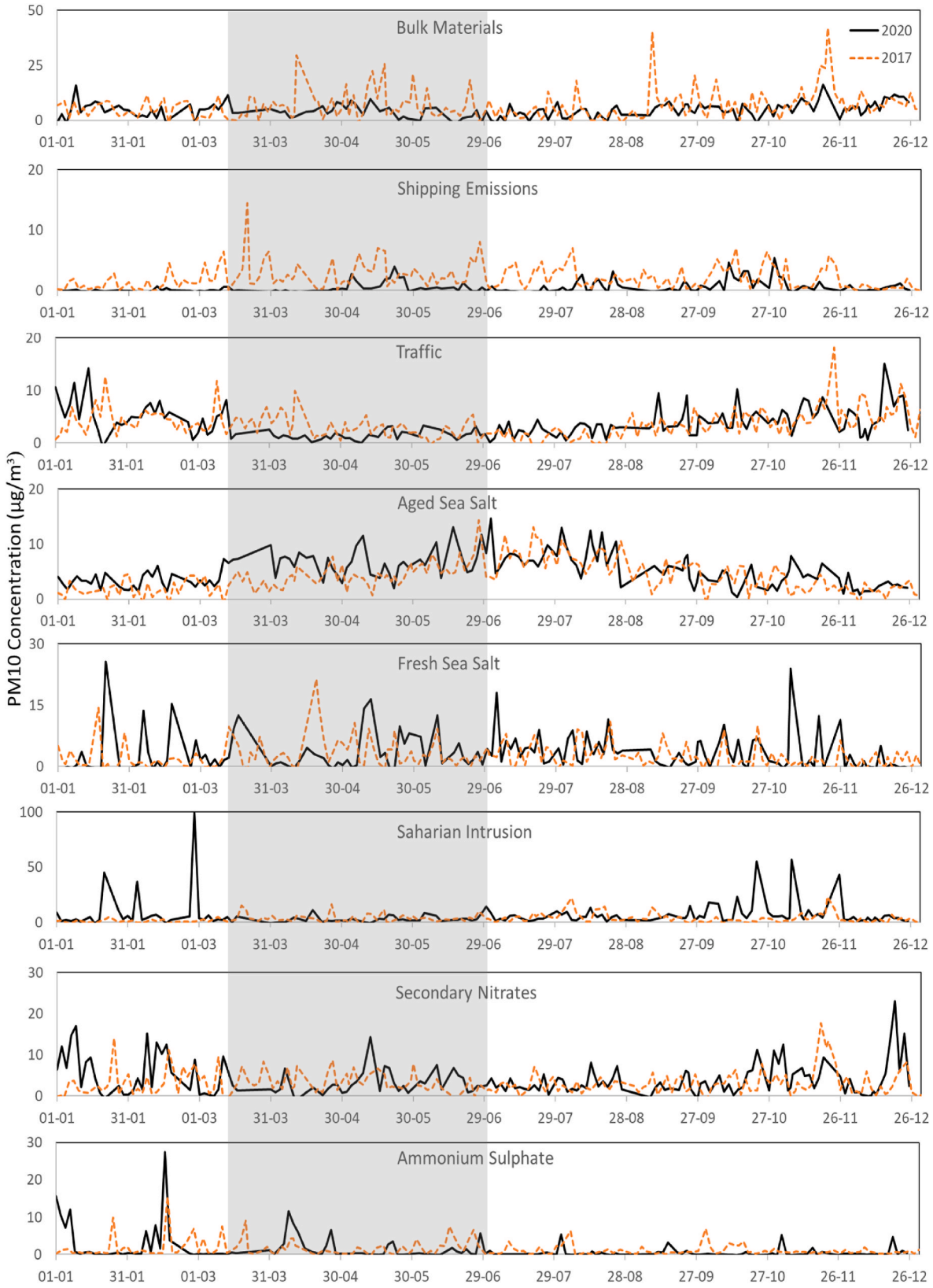

Fig. 4. Temporal evolution of the contribution to PM_{10} of each factor in the two periods of study. 2017 dotted and 2020 continuous line. The shaded area represents the lockdown period.

In summer, at higher temperatures, the mixing layer is wider and stratified in the area of study, lowering the levels of nitrate aerosols (Navarro-Selma et al., 2022).

3.2.8. Ammonium sulfate

This factor represents only 5% of the total PM_{10} (1.3 μg/m^3) and is very well defined, containing almost exclusively NH_4^+(91%) and SO_4^{2-}(9%). The low contribution of this factor is mainly due to the low availability of ammonia in the study zone. This is due to the few sources of ammonia present in the study area, thus indicating a possible regional origin of this source.

4. Comparison between periods

4.1. Lockdown effects at annual scale (annual differences)

In this section, the concentrations of different sources will be compared between 2017 and 2020 for the entire year, including the prelockdown period, the lockdown period and the gradual recovery of activity. The objective is to evaluate the impact that the COVID-19 had on the PM_{10} average annual concentrations of the different sources. The average annual contribution of the factors, in both years are compared in Fig. 5. Factors with statistically significant differences are marked with an '*'.

As has been already mentioned, the annual PM_{10} concentration obtained for both periods was the same. Regarding the sources, a significant difference was observed between the two periods for the Shipping emissions, Saharan intrusions, and Ammonium sulfate factors. (Fig. 5).

In the case of the Shipping factor, the significant reduction (77%) is due to the abrupt drop in marine traffic, particularly in relation to the transport of passengers on cruise ships since the beginning of the year. The number of cruise ships docking at the port of Alicante decreased considerably, going from 43 cruises with 63.088 passengers in 2017 to a single cruise with 2.413 passengers in 2020. As can be seen in Fig. 4, sporadic emissions started to reappear with spring-summer E-SE winds and towards the end of the year with the relaxation of the COVID-19 measures. On the other hand, this reduction is probably greater due to the effect of the IMO 2020 limiting the sulfur in fuel-oils to 0.5% m/m, which could lead to a more substantial reduction throughout the whole year 2020 as fuel-oil is the main fuel used by ships.

The Saharan intrusion has a significant increase during 2020 compared to the reference year (2017), doubling its concentration during 2020 and having a large impact during the months of January, February, October and November (Fig. 4). On the other hand, the Saharan intrusion episodes during 2017 have a more homogeneous distribution along the year. The increase of this factor is the main reason why the total PM_{10} concentration in 2020 remains similar to the reference year despite the measures taken during the pandemic.

Although the reduction in the average ammonium sulfate source concentration is only 0.1 μg/m^3, the difference compared to 2017 is significant. This is because the concentration patterns are different in 2020 compared to 2017. As can be seen in Fig. 4, during 2020 the ammonium sulfate source consists of a few days of high concentration followed by periods where no ammonium sulfate was detected. During 2017 on the other hand, days with moderate amounts of ammonium sulfate were more frequent. This source probably depends on medium to long range transport which would explain its temporal distribution.

The annual difference in the Bulk Material factor (1.9 μg/m^3) between both years was not considered significant according to the test. Bulk charge operations continued during the COVID period, indicating that most of the variation in the Bulk Material factor was attributed to changes in the port's operational methodology and meteorology. No significant effects of the applied abatement techniques on this source were observed on an annual scale. Further measures are planned to be implemented in the port, as managing loading of most dusty materials in an enclosed facility and the use of containers for the transport of some pulverulent materials.

4.2. The effects of the lockdown

The lockdown effect was addressed by comparing the average contribution of the factors in the period from March to June 2020 (lockdown period) with the same period in 2017. Fig. 6 shows the contribution of the 8 different factors during both March to June periods. In the Figure, factors with statistically relevant differences are marked with an '*'.

Unlike at the annual scale, Traffic sources exhibited significant reductions during 2020 lockdown period (39% reduction). On the other hand, Shipping emissions sources remained significant both during the lockdown period (84%) and throughout the entire year. During the 2020 lockdown period there were no cruises reaching the port and therefore the contribution of Shipping emission sources decreased dramatically. Maritime transport of goods, on the other hand, did not show such a reduction as it was mainly raw matter needed for local industry.

To emphasize on the effect of the COVID-19 lockdown on traffic, the 2020 daily evolution of the traffic source has been plotted with the NO_2 levels and the daily number of cars on the largest and closest main road to the sampling area (Fig. 7).

The reduction in cars observed in the COVID period coincides with the temporal evolution of the traffic factor and also with the daily NO_2 levels. During the COVID period, the OC/EC ratio reversed the annual trend saw in section 3.1 and exhibited the highest values of the year, aligning with the reduction in traffic emissions. The rapid recovery of the number of cars after the lockdown explains the significant differences within the year 2020 (lockdown period and the whole year). However, as we saw in the previous section, even though the number of cars was 28% lower than in 2017, there was no reduction in the PM_{10} levels associated with the traffic factor in 2020. This would indicate that meteorology may play a key role in compensating for reductions in sources. An increase in the number of accumulation episodes, for example, would compensate for a significant reduction in the number of cars on the road.

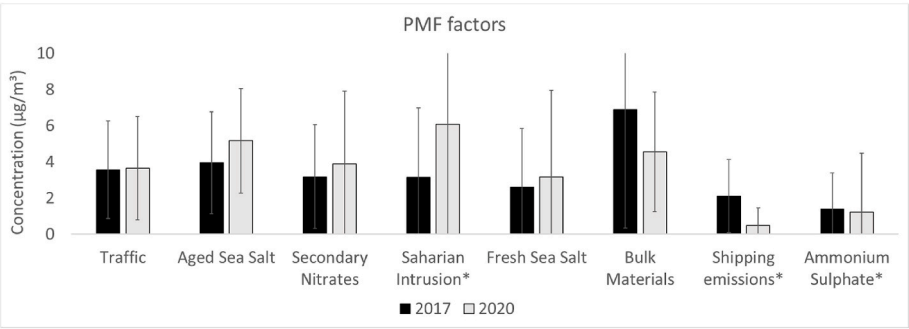

Fig. 5. PMF factor contribution in the two years of study (μg/m^3). The bars represent the standard deviation of the factor.

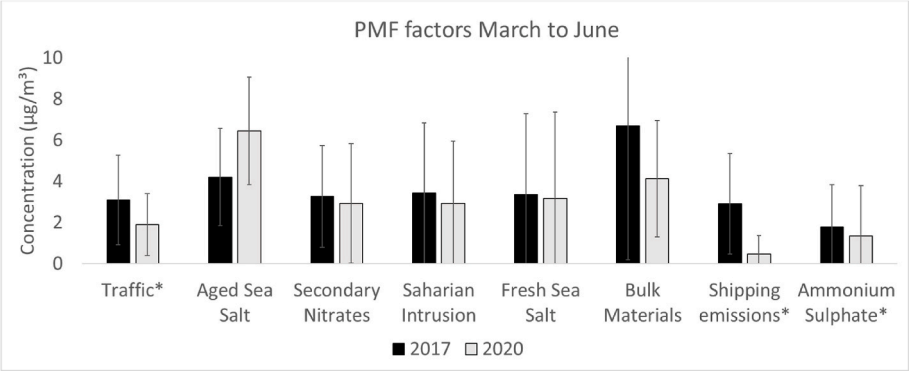

Fig. 6. PMF factor contribution during the lockdown months compared to the same months in the period 2017 (µg/m^3). The bars represent the standard deviation of the factor.

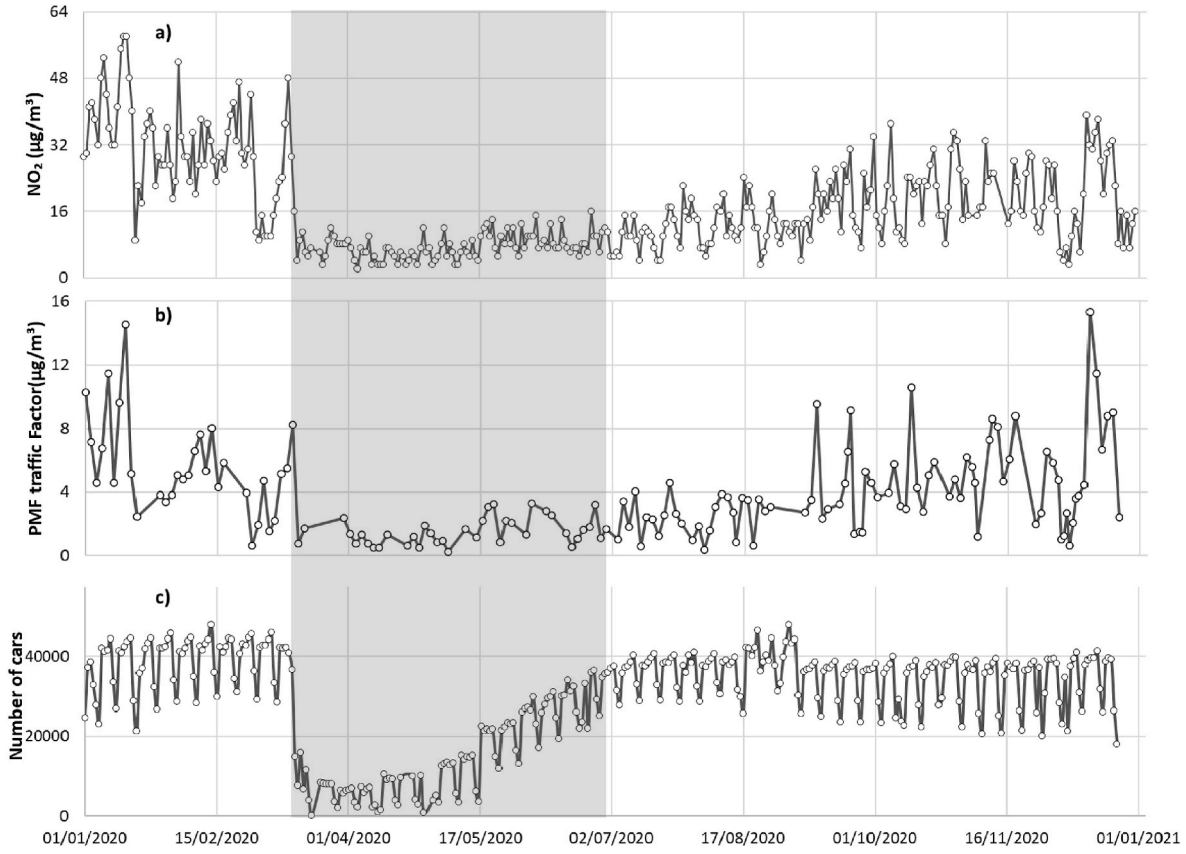

Fig. 7. a) NO_2 at the closest air quality station, b) PMF traffic factor and c) Daily number of cars during 2020. The shaded area represents the lockdown period.

4.3. *Comparison of sources causing PM_{10} daily exceedances of 50 µg/m^3*

As mentioned before, the annual mean in 2020 and the number of exceedances of the daily limit value of 50 µg/m^3 are very similar to that of the reference year (7 in 2020 and 8 in 2017). Fig. 8 shows the contribution of the factors influencing PM_{10} concentration levels on exceedance days in 2020 and during the reference period. The anthropogenic factors traffic and bulk material, and Saharan intrusion factor are presented separately and secondary sources or sources with a minor contribution are shown grouped together. As can be seen, the contribution of the sources to the excess days differs significantly between the two years.

The contribution of the Saharan factor to the annual average was 6.1 µg/m^3 in 2020 compared to 3.2 µg/m^3 in 2017. In a scenario with no Saharan intrusions, the threshold limit would not be exceeded on any day, i.e. the 7 exceedances of this limit would disappear. If the same is done for 2017, only half of the exceedances would disappear (4 out of 8), indicating the importance of anthropogenic sources (as handling of bulk material) that considerably contribute to PM_{10} exceedances, especially in 2017.

If the same type of analysis is performed with the source related to bulk movement, a reduction of the exceedances from 8 to 1 in 2017 is achieved. Only two exceedances could be avoided in 2020 by reducing this source. The reduction of the bulk source contribution in the daily exceedances in 2020 is mainly related to the implementation of mitigation measures and not directly to the pandemic itself. Fig. 4 shows the change in temporal evolution in both years, highlighting the disappearance of concentration peaks due to the complementary abatement

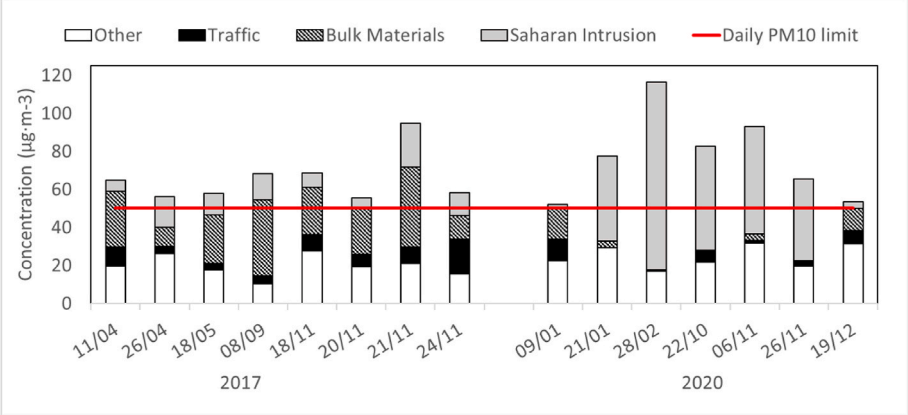

Fig. 8. Contribution of the different sources to the daily exceedances of 50 µg/m^3.

techniques and a halt in activity when concentrations exceeded a certain threshold.

In a scenario with a drastic reduction in the traffic source, two of the excess days in both years could be avoided. This indicates that the impact of the traffic source on daily exceedances has not changed between 2020 and 2017 and that the significant reduction of this source during the lockdown months has not affected the number of exceedances in 2020.

5. Conclusions

A source apportionment with PMF was performed to quantify the effect COVID-19 had in PM_{10} particle levels at the port-city boundary of Alicante. The mean PM_{10} concentration in 2020, COVID year, was 29.1 ± 17.8 µg/m^3, not statistically different from the mean obtained at the same sampling point during the reference period. Likewise, the number of days above 50 µg/m^3 was very similar.

Among the sources related to port activity, only the source representing fuel-oil burning emissions experienced a significant reduction (84% reduction during the lockdown period and 77% reduction throughout the whole year). This reduction was primarily due to the decrease in the number of ships arriving at the port during the pandemic and, to a lesser extent, the implementation of IMO 2020 regulations. However, the source representing bulk material handling emissions showed no variation in both periods. The application of complementary mitigation techniques by the port authority has resulted in a reduction in the number of exceedances despite no change in the average annual contribution.

In the case of the traffic source, in 2020, the difference in the concentration between the lockdown period and the same months in 2017 is 39%. This reduction coincides with a reduction in the number of cars circulating close to the sampling station and with a reduction in the NO_2 concentrations. However, the traffic source does not show any difference in the port on an annual scale contributing 3.6 µg/m^3 and 3.7 µg/m^3 during 2017 and 2020 respectively. Despite the reduction of this source during the lockdown, concentrations increased for the remainder of the year, offsetting the effect it could have had on an annual scale.

Reductions caused by the pandemic have been compensated by natural and secondary sources such as Saharan intrusion, fresh sea salt and aged sea salt, which combined increased from 36% to 51% of PM_{10} concentration from 2017 to 2020. Therefore, in absence of the COVID-19 effect PM_{10} levels would have been higher in 2020 than in the reference year.

CRediT authorship contribution statement

D. Tobarra: Conceptualization, Validation, Formal analysis, Investigation, Data curation, Writing – original draft, Writing – review & editing, Visualization. **E. Yubero:** Conceptualization, Methodology, Writing – review & editing. **Á. Clemente:** Conceptualization, Methodology, Resources, Writing – review & editing, Visualization, Supervision, Project administration, Funding acquisition. **A. Carratala:** Validation, Investigation.

Declaration of competing interest

The authors declare that they have no known competing financial interests or personal relationships that could have appeared to influence the work reported in this paper.

Data availability

Data will be made available on request.

Funding/Acknowledgments

This work has been carried out within the framework of the doctoral program of the University of Alicante in collaboration with companies (UAIND-17-1A). The authors want to express their gratitude to the Alicante Port Authority for their participation in this program with the project (PUERTOALICANTE1-20Y), which together with the University of Alicante provided the funding for the sampling and the PhD grant.

References

Alastuey, A., Moreno, N., Querol, X., Viana, M., Artíñano, B., Luaces, J.A., Basora, J., Guerra, A., 2007. Contribution of harbour activities to levels of particulate matter in a harbour area: hada project-Tarragona Spain. Atmos. Environ. 41 (1994), 6366–6378.

Amato, F., Pandolfi, M., Escrig, A., Querol, X., Alastuey, A., Pey, J., Perez, N., Hopke, P. K., 2009. Quantifying road dust resuspension in urban environment by multilinear engine: a comparison with PMF2. Atmos. Environ. 43 (1994), 2770–2780.

Autoridad Portuaria de Alicante, 2021. 2020 Alicante Port Annual Report Autoridad Portuaria de Alicante.

Belis, C.A., Larsen, B.R., Amato, F., El Haddad, I., Favez, O., Harrison, R.M., Hopke, P.K., Nava, S., Paatero, P., Prevot, A., Quass, U., Vecchi, R., Viana, M., 2014. European Guide on Air Pollution Source Apportionment with Receptor Models. European Union.

Cardoso, J., Almeida, S.M., Nunes, T., Almeida-Silva, M., Cerqueira, M., Alves, C., Rocha, F., Chaves, P., Reis, M., Salvador, P., Artinano, B., Pio, C., 2018. Source apportionment of atmospheric aerosol in a marine dusty environment by ionic/composition mass balance (IMB). Atmos. Chem. Phys. 18, 13215–13230.

Cheng, Z., Jiang, J., Fajardo, O., Wang, S., Hao, J., 2013. Characteristics and health impacts of particulate matter pollution in China (2001–2011). Atmos. Environ. 65 (1994), 186–194.

Clemente, Á., Yubero, E., Galindo, N., Crespo, J., Nicolás, J.F., Santacatalina, M., Carratala, A., 2021. Quantification of the impact of port activities on PM_{10} levels at the port-city boundary of a mediterranean city. J. Environ. Manag. 281, 111842.

Clemente, Á., Yubero, E., Nicolás, J.F., Caballero, S., Crespo, J., Galindo, N., 2022. Changes in the concentration and composition of urban aerosols during the COVID-19 lockdown. Environ. Res. 203, 111788.

Collivignarelli, M.C., Abbà, A., Bertanza, G., Pedrazzani, R., Ricciardi, P., Carnevale Miino, M., 2020. Lockdown for CoViD-2019 in Milan: what are the effects on air quality? Sci. Total Environ. 732, 139280.
Comero, S., Capitani, L., Gawlik, B.M., 2009. Positive matrix factorisation (PMF). EUR. Scientific and Technical Research Series 23946.
Dantas, G., Siciliano, B., França, B.B., da Silva, C.M., Arbilla, G., 2020. The impact of COVID-19 partial lockdown on the air quality of the city of Rio de Janeiro, Brazil. Sci. Total Environ. 729, 139085.
Galindo, N., Yubero, E., 2017. Day-night variability of water-soluble ions in PM_{10} samples collected at a traffic site in southeastern Spain. Environ. Sci. Pollut. Res. Int. 24, 805–812.
Galindo, N., Yubero, E., Nicolás, J.F., Varea, M., Crespo, J., 2018a. Characterization of metals in PM1 and PM_{10} and health risk evaluation at an urban site in the western mediterranean. Chemosphere 201, 243–250.
Galindo, N., Yubero, E., Nicolás, J.F., Varea, M., Clemente, Á., 2018b. Day-night variability of PM_{10} components at a mediterranean urban site during winter. Air Quality, Atmosphere Health 11, 1251–1258.
Gayen, A., Haque, S.M., Mishra, S.V., 2021. COVID-19 induced lockdown and decreasing particulate matter (PM_{10}): an empirical investigation of an asian megacity. Urban Clim. 36, 100786.
Grigoratos, T., Martini, G., 2014. Non-Exhaust Traffic Related Emissions – Brake and Tyre Wear PM.
Huang, X.H.H., Ip, H.S.S., Yu, J.Z., 2011. Secondary organic aerosol formation from ethylene in the urban atmosphere of Hong Kong: a multiphase chemical modeling study. J. Geophys. Res. 116 n/a.
Jaeckels, J.M., Bae, M., Schauer, J.J., 2007. Positive matrix factorization (PMF) analysis of molecular marker measurements to quantify the sources of organic aerosols. Environ. Sci. Technol. 41, 5763–5769.
Johnson, N.M., Hoffmann, A.R., Behlen, J.C., Lau, C., Pendleton, D., Harvey, N., Shore, R., 2021. Air pollution and children's health—a review of adverse effects associated with prenatal exposure from fine to ultrafine particulate matter. Environ. Health Prev. Med. 26, 72.
Khaniabadi, Y., Daryanoosh, S.M., Hopke, P.K., Ferrante, M., De Marco, A., Sicard, P., Oliveri Conti, G., Goudarzi, G., Basiri, H., Mohammadi, M.J., Keishams, F., 2017. Acute myocardial infarction and COPD attributed to ambient SO2 in Iran. Environ. Res. 156, 683–687.
Kim, E., Hopke, P.K., 2008. Source characterization of ambient fine particles at multiple sites in the Seattle area. Atmos. Environ. 42 (1994), 6047–6056.
Kim, E., Hopke, P.K., Larson, T.V., Maykut, N.N., Lewtas, J., 2004. Factor analysis of Seattle fine particles. Aerosol. Sci. Technol. 38, 724–738.
Larsen, R.K., Baker, J.E., 2003. Source apportionment of polycyclic aromatic hydrocarbons in the urban atmosphere: a comparison of three methods. Environ. Sci. Technol. 37, 1873–1881.
Ledoux, F., Roche, C., Cazier, F., Beaugard, C., Courcot, D., 2018. Influence of ship emissions on NOx, SO2, O3 and PM concentrations in a north-sea harbor in France. J. Environ. Sci. 71, 56–66.
Lee, E., Chan, C.K., Paatero, P., 1999. Application of positive matrix factorization in source apportionment of particulate pollutants in Hong Kong. Atmos. Environ. 33 (1994), 3201–3212.
Ma, Q., Jia, P., She, X., Haralambides, H., Kuang, H., 2021. Port integration and regional economic development: lessons from China. Transport Pol. 110, 430–439.
Mahapatra, B., Walia, M., Avis, W., Saggurti, N., 2020. Effect of exposure to PM_{10} on child health: evidence based on a large-scale survey from 184 cities in India. BMJ Glob. Health 5.
Massimi, L., Pietrodangelo, A., Frezzini, M.A., Ristorini, M., De Francesco, N., Sargolini, T., Amoroso, A., Di Giosa, A., Canepari, S., Perrino, C., 2022. Effects of COVID-19 lockdown on PM_{10} composition and sources in the Rome area (Italy) by elements' chemical fractionation-based source apportionment. Atmos. Res. 266, 105970.
Maykut, N.N., Lewtas, J., Kim, E., Larson, T.V., 2003. Source apportionment of $PM_{2.5}$ at an urban IMPROVE site in Seattle, Washington. Environ. Sci. Technol. 37, 5135–5142.
Megido, L., Negral, L., Castrillón, L., Marañón, E., Fernández-Nava, Y., Suárez-Peña, B., 2016. Traffic tracers in a suburban location in northern Spain: relationship between carbonaceous fraction and metals. Environ. Sci. Pollut. Control Ser. 23, 8669–8678.
Merico, E., Gambaro, A., Argiriou, A., Alebic-Juretic, A., Barbaro, E., Cesari, D., Chasapidis, L., Dimopoulos, S., Dinoi, A., Donateo, A., Giannaros, C., Gregoris, E., Karagiannidis, A., Konstandopoulos, A.G., Ivošević, T., Liora, N., Melas, D., Mifka, B., Orlić, I., Poupkou, A., Sarovic, K., Tsakis, A., Giua, R., Pastore, T., Nocioni, A., Contini, D., 2017. Atmospheric impact of ship traffic in four adriatic-ionian port-cities: comparison and harmonization of different approaches. Transport. Res. Transport Environ. 50, 431–445.
Millán-Martínez, M., Sánchez-Rodas, D., Sánchez de la Campa, A.M., Alastuey, A., Querol, X., de la Rosa, J.D., 2021. Source contribution and origin of PM_{10} and arsenic in a complex industrial region (Huelva, SW Spain). Environ. Pollut. 274 (1987), 116268.
Millán-Martínez, M., Sánchez-Rodas, D., Sánchez de la Campa, A.M., de la Rosa, J., 2022. Impact of the SARS-CoV-2 lockdown measures in southern Spain on PM_{10} trace element and gaseous pollutant concentrations. Chemosphere 303, 134853.
Nauwelaerts, S.J.D., Van Goethem, N., Ureña, B.T., De Cremer, K., Bernard, A., Saenen, N.D., Nawrot, T.S., Roosens, N.H.C., De Keersmaecker, S.C.J., 2022. Urinary CC16, a potential indicator of lung integrity and inflammation, increases in children after short-term exposure to $PM_{2.5}/PM_{10}$ and is driven by the CC16 38GG genotype. Environ. Res. 212, 113272.
Navarro-Selma, B., Clemente, A., Nicolás, J.F., Crespo, J., Carratalá, A., Lucarelli, F., Giardi, F., Galindo, N., Yubero, E., 2022. Size segregated ionic species collected in a harbour area. Chemosphere 294, 133693.
Notteboom, T.E., Pallēs, A.A., Rodrigue, J., 2022. Port Economics, Management and Policy. Routledge, London; New York.
Oduber, F., Calvo, A.I., Castro, A., Blanco-Alegre, C., Alves, C., Calzolai, G., Nava, S., Lucarelli, F., Nunes, T., Barata, J., Fraile, R., 2021. Characterization of aerosol sources in León (Spain) using positive matrix factorization and weather types. Sci. Total Environ. 754, 142045.
Paatero, P., Hopke, P.K., 2003. Discarding or downweighting high-noise variables in factor analytic models. Anal. Chim. Acta 490, 277–289.
Paatero, P., Tapper, U., 1994. Positive matrix factorization: a non-negative factor model with optimal utilization of error estimates of data values. Environmetrics 5, 111–126.
Pandolfi, M., Gonzalez-Castanedo, Y., Alastuey, A., de la Rosa, J.D., Mantilla, E., de la Campa, A.S., Querol, X., Pey, J., Amato, F., Moreno, T., 2010. Source apportionment of PM_{10} and $PM_{2.5}$ at multiple sites in the strait of Gibraltar by PMF: impact of shipping emissions. Environ. Sci. Pollut. Res. Int. 18, 260–269.
Pant, P., Harrison, R.M., 2013. Estimation of the contribution of road traffic emissions to particulate matter concentrations from field measurements: a review. Atmos. Environ. 77 (1994), 78–97.
Pérez, N., Pey, J., Reche, C., Cortés, J., Alastuey, A., Querol, X., 2016. Impact of harbour emissions on ambient PM_{10} and $PM_{2.5}$ in Barcelona (Spain): evidence of secondary aerosol formation within the urban area. Sci. Total Environ. 571, 237–250.
Polissar, A.V., Hopke, P.K., Paatero, P., Malm, W.C., Sisler, J.F., 1998. Atmospheric aerosol over Alaska: 2. elemental composition and sources. J. Geophys. Res. Atmos. 103, 19045–19057.
Russo, M.A., Leitão, J., Gama, C., Ferreira, J., Monteiro, A., 2018. Shipping emissions over Europe: a state-of-the-art and comparative analysis. Atmos. Environ. 177 (1994), 187–194.
Santacatalina, M., Reche, C., Minguillón, M.C., Escrig, A., Sanfelix, V., Carratalá, A., Nicolás, J.F., Yubero, E., Crespo, J., Alastuey, A., Monfort, E., Miró, J.V., Querol, X., 2010. Impact of fugitive emissions in ambient PM levels and composition : a case study in southeast Spain. Sci. Total Environ. 408, 4999–5009.
Santacatalina, M., Carratalá, A., Mantilla, E., 2011. Influence of local and regional mediterranean meteorology on SO2 ground-level concentrations in SE Spain. J. Environ. Monit. 13, 1634–1645.
Sasmita, S., Kumar, D.B., Priyadharshini, B., 2022. Assessment of sources and health impacts of PM_{10} in an urban environment over eastern coastal plain of India. Environ. Chall. 7, 100457.
Sharma, S.K., Mandal, T.K., Saxena, M., Rashmi, Sharma, A., Datta, A., Saud, T., 2014. Variation of OC, EC, WSIC and trace metals of PM_{10} in Delhi, India. J. Atmos. Sol. Terr. Phys. 113, 10–22.
Sharma, S., Zhang, M., Anshika Gao, J., Zhang, H., Kota, S.H., 2020. Effect of restricted emissions during COVID-19 on air quality in India. Sci. Total Environ. 728, 138878.
Shukla, S., Khan, R., Saxena, A., Sekar, S., Ali, E.F., Shaheen, S.M., 2022. Appraisal of COVID-19 lockdown and unlocking effects on the air quality of north India. Environ. Res. 204, 112107.
Song, C.H., Carmichael, G.R., 1999. The aging process of naturally emitted aerosol (sea-salt and mineral aerosol) during long range transport. Atmos. Environ. 33 (1994), 2203–2218.
Strak, M., Steenhof, M., Godri, K.J., Gosens, I., Mudway, I.S., Cassee, F.R., Lebret, E., Brunekreef, B., Kelly, F.J., Harrison, R.M., Hoek, G., Janssen, N.A.H., 2011. Variation in characteristics of ambient particulate matter at eight locations in The Netherlands – the RAPTES project. Atmos. Environ. 45 (1994), 4442–4453.
Szidat, S., Jenk, T.M., Synal, H., Kalberer, M., Wacker, L., Hajdas, I., Kasper-Giebl, A., Baltensperger, U., 2006. Contributions of fossil fuel, biomass-burning, and biogenic emissions to carbonaceous aerosols in zurich as traced by 14C. J. Geophys. Res. Atmos. 111, D07206–n/a.
Vecchi, R., Chiari, M., D'Alessandro, A., Fermo, P., Lucarelli, F., Mazzei, F., Nava, S., Piazzalunga, A., Prati, P., Silvani, F., Valli, G., 2008. A mass closure and PMF source apportionment study on the sub-micron sized aerosol fraction at urban sites in Italy. Atmos. Environ. 42 (1994), 2240–2253.
Viana, M., Amato, F., Alastuey, A., Querol, X., Moreno, T., García Dos Santos, S., Herce, M.D., Fernández-Patier, R., 2009. Chemical tracers of particulate emissions from commercial shipping. Environ. Sci. Technol. 43, 7472–7477.
World Health Organization, 2021. WHO Global Air Quality Guidelines. Particulate Matter ($PM_{2.5}$ and PM_{10}), Ozone, Nitrogen Dioxide, Sulfur Dioxide and Carbon Monoxide. World Health Organization, Geneva, 2021. Licence: CC BY-NC-SA 3.0 IGO.
Wu, G., Du, X., Wu, X., Fu, X., Kong, S., Chen, J., Wang, Z., Bai, Z., 2013. Chemical composition, mass closure and sources of atmospheric PM_{10} from industrial sites in Shenzhen, China. J. Environ. Sci. 25, 1626–1635.
Wu, S., Cai, M., Xu, C., Zhang, N., Zhou, J., Yan, J., Schwab, J.J., Yuan, C., 2020. Chemical nature of $PM_{2.5}$ and PM_{10} in the coastal urban Xiamen, China: insights into the impacts of shipping emissions and health risk. Atmos. Environ. 227 (1994), 117383.
Xu, K., Cui, K., Young, L., Wang, Y., Hsieh, Y., Wan, S., Zhang, J., 2020. Air quality index, indicatory air pollutants and impact of COVID-19 event on the air quality near central China. Aerosol Air Qual. Res. 20, 1204–1221.
Yubero, E., Carratalá, A., Crespo, J., Nicolás, J., Santacatalina, M., Nava, S., Lucarelli, F., Chiari, M., 2010. PM_{10} source apportionment in the surroundings of the San Vicente del Raspeig cement plant complex in southeastern Spain. Environ. Sci. Pollut. Res. Int. 18, 64–74.

Yubero, E., Galindo, N., Nicolás, J.F., Crespo, J., Calzolai, G., Lucarelli, F., 2015. Temporal variations of PM1 major components in an urban street canyon. Environ. Sci. Pollut. Res. Int. 22, 13328–13335.

Zabalza, J., Ogulei, D., Hopke, P.K., Jong, Hoon Lee, Hwang, I., Querol, X., Alastuey, A., Santamaria, J.M., 2006. Concentration and sources of PM_{10} and its constituents in Alsasua, Spain. Water Air Soil Pollut. 174, 385–404.

Zhou, Y., Huang, X., Bian, Q., Griffith, S., Louie, P., Yu, J., 2015. Sources and atmospheric processes impacting oxalate at a suburban coastal site in Hong Kong: insights inferred from 1 year hourly measurements. J. Geophys. Res. Atmos. 120, 9772–9788.

Žitnik, M., Jakomin, M., Pelicon, P., Rupnik, Z., Simčič, J., Budnar, M., Grlj, N., Marzi, B., 2005. Port of koper-elemental concentrations in aerosols by PIXE. X Ray Spectrom. 34, 330–334.